JOURNAL OF SOLID STATE CHEMISTRY 1, 19–27 (1969)

On the Band Structure of Rare Earth Chalcogenides and Pnictides†

J. M. HONIG

Department of Chemistry, Purdue University, West Lafayette, Indiana 47907

Received December 21, 1968

Using LCAO-tight bonding methodology the band structure of rare earth chalcogenides and pnictides is determined under a variety of simplifying conditions. The analysis shows that one cannot in general separate cation–cation from cation–anion–cation interactions. Schematic energy band diagrams based on the secular determinantal equation are presented for directions of high symmetry in reciprocal space. These are used to rationalize the observed metallic or semiconducting properties of the rare earth chalcogenides and pnictides.

1. Introduction

This paper deals with the problem of developing a qualitative band structure scheme for the rare earth chalcogenides (excepting the oxides) and pnictides; as indicated in recent reviews (*1*, *2*), their electrical properties are under active investigation. The fact that these materials are either metallic or semiconducting calls for the use of band models in the interpretation of their electrical characteristics. Considerable emphasis will be placed on the systematic exploitation of the LCAO-tight binding methodology to achieve this aim.

Early attempts (*6*, *7*) to interpret the electrical properties of this class of materials were based on Pauling's approach involving resonating bond structures. Later interpretations (*8–11*) corresponded more closely to the zone theory of metals, but the various investigators referred only vaguely to what they termed 5*d* or 6*s* bands, and were concerned more with a description of the transport phenomena than with band structures.

Studies by Bilz (*4*) and Goodenough (*12*) have dealt with the characterization of band structures for materials crystallizing in the rocksalt structure. However, neither publication addressed itself to the problem discussed below, and the approach as well as some of the conclusions are different.

The analysis offered here is restricted to the range above any magnetic ordering temperature in the lanthanon chalcogenides or pnictides; this sidesteps various complications arising from magnetic ordering effects.

† This work was supported through NSF Grant GP 8302.

2. Fundamentals

The LCAO-tight binding scheme represents a convenient analytical tool for determining the band structure of any solid from its crystal structure; details may be found in publications by Slater and Koster (*3*) and by others (*5*, *13*). Following their methodology, the band structure will be set up subject to several important restrictions: (1) The choice of basis functions will be limited to the 5*d*, 6*s*, 6*p* orbitals of the lanthanons (hereafter designated by the symbol Ln) and to the *ns* and *np* orbitals of the chalcogen or pnicogen (hereafter designated as X, excluding the oxides). (2) The 4*f* states will be considered as noninteracting and thus, as nonbonding states. (3) Interactions among atoms in the rocksalt lattice will be restricted to nearest neighbors (Ln–X type interactions) and to next-nearest neighbors among the cations and anions (Ln–Ln and X–X type interactions). (4) Any effects arising from the existence of lattice defects or nonstoichiometry will be ignored; spin-orbit effects are also left out of account.

In the LCAO-tight binding approximation information on the band structure is conveyed through a secular determinantal equation of the form

$$|\langle b_{l'j'}|\mathbf{H}-\epsilon|\, b_{lj}\rangle| = 0.$$

Here, **H** is the Hamiltonian operator, for one electron in the crystal lattice, ϵ is the one-electron energy, and $b_{l'j'}$ or b_{lj} represent the Bloch functions appropriate for a description of the wave functions for electrons in a periodic lattice structure. Further, j' and j designate the distinct types of atoms in the

lattice, while $l'_{j'}$ and l_j index the atomic orbitals used to construct the Bloch functions. When this construction is carried through one obtains the secular determinantal equation in the form

$$\left|\sum_{\mathbf{q}} S_{j'j}(\mathbf{k},\mathbf{q})[\langle l'_{j'}|\,\mathbf{H}|l_j(\mathbf{q})\rangle - \epsilon\langle l'_{j'}|\,l_j(\mathbf{q})\rangle]\right| \equiv \left|\sum_{\mathbf{q}} S_{j'j}(\mathbf{k},\mathbf{q})\,E_{l'_{j'}l_j}(\mathbf{q})\right| = 0$$

In the above, E is a parameter expressed in terms of the transfer integral $\langle l'_{j'}|\,\mathbf{H}|l_j(\mathbf{q})\rangle$ and the overlap integral $\langle l'_{j'}|\,l_j(\mathbf{q})\rangle$ involving the atomic orbitals as basis functions. S is a corresponding structure factor which contains appropriate exponential phase factors or trigonometric terms in the wave number vector $\mathbf{k}$ for the electron. The triplet $\mathbf{q} \equiv (q_1,q_2,q_3)$ pertains to the relative orientation of atoms in the lattice as detailed below. The solution of the secular determinantal equation, when expressed in the functional form $\epsilon(\mathbf{k})$, specifes the dispersion relations or the band structure for the crystal.

Under assumptions (1)–(3), j and j' designate either the Ln ($j,j' = \mathrm{c}$) or X ($j,j' = \mathrm{a}$) atoms. The l'_c and l_c index the cationic wave functions s_c, p_c $(x_\mathrm{c},y_\mathrm{c},z_\mathrm{c})$, $e_\mathrm{g}(x^2-y^2,z^2)$, and $t_{2\mathrm{g}}(xy,xz,yz)$; l'_a and l_a index the anionic wave functions s_a and $p_\mathrm{a}(x_\mathrm{a},y_\mathrm{a},z_\mathrm{a})$.

The exact form of the secular equation is unimportant for the present; one should note, however, that with the orbitals selected earlier, one obtains a 13×13 secular determinant whose nonvanishing entries indicate which types of atomic orbitals interact in the formation of bands. Furthermore, from the nature of the transfer and overlap integrals one can decide whether any given interaction is of σ, π, δ, or mixed character. Where by reason of incompatible symmetry the transfer or overlap integral between two centers is zero, the corresponding entry in the secular determinantal equation vanishes identically. All remaining entries generally depend on $\mathbf{k}$; along directions of high symmetry in reciprocal space, however, some structure factors $S_{j'j}$ may also vanish identically, in which case the secular determinantal equation simplifies further.

The nonvanishing entries of the secular determinant may be set up by examining the appropriate parts of Table II in Ref. (*3*) in light of the above discussion. One should be aware of minor differences in the set of basis functions employed by Slater and Koster and those used here.† As a result, the symbol $E_{l'_{j'}l_j}(\mathbf{q})$, which designates only the transfer integral in Ref. (*3*), denotes the more complex function enclosed in square brackets in the above secular determinantal equation, including the quantity ϵ. This explains why the energy parameter appears nowhere explicitly in the tabulations provided below. In now considering all Ln–Ln or X–X interactions, a given Ln or X atom in the crystal is surrounded by twelve others of the same kind whose location relative to the atom under study is specified by the (110) Miller indices. Hence, one must pick out from the tabulation all entries with the $E(000)$ or $E(110)$ labels. As regards the Ln–X or X–Ln interactions, a given Ln or X atom in the crystal is surrounded octahedrally by nearest neighbors of the opposite type, whose location relative to the atom under study is specified by the (100) Miller indices. Here one must pick out from the tables all entries associated with $E(000)$ or $E(100)$. The trigonometric factors in these tabulations that occur with a given E symbol represent the quantities $S_{j'j}$. In the present study the number of E parameters exceeds that specified in Ref. (*3*), all of which pertain to atoms of a given type. Here, there is one set $E_{l'_\mathrm{c}l_\mathrm{c}}$ for Ln–Ln interactions, a second set $E_{l'_\mathrm{a}l_\mathrm{a}}$ for X–X interactions and two sets $E_{l'_\mathrm{a}l_\mathrm{c}}$ and $E_{l'_\mathrm{c}l_\mathrm{a}} = E_{l_\mathrm{a}l'_\mathrm{c}}{}^*$ for X–Ln and Ln–X interactions. Nonvanishing entries missing from the table may be constructed by the "method of advancing the indices" as explained in the article. The secular determinantal equation constructed in this manner must be hermitian. Finally, the effect of the $4f$ orbitals on the binding scheme must be considered separately.

Unfortunately, the 13×13 secular determinantal equation constructed in accord with the above commentary is exceedingly complex: It contains 152 nonvanishing elements characterized by 36 distinct E parameters. As a consequence, all elements are interconnected and all types of interactions are scrambled; thus, one cannot distinguish bands arising from σ-type or π-type interactions, nor is it possible to separate out the effects of direct cation–cation or anion–anion orbital overlap from the effects due to cation–anion interactions. The schemes suggested by Bilz (*4*) and Goodenough (*12*) must therefore correspond to lower levels of approximation in the LCAO-tight binding scheme. Some of these are examined in the next section.

3. Approximation Schemes

The first problem taken up here deals with the possibility of splitting the bands into a subset

† The basis functions used by Slater and Koster are orthogonalized atomic orbitals, which have the virtue of eliminating most of the overlap integrals, since under their use, $\langle l'_{j'}|\,l_j\rangle = \delta(l'_{j'},l_j)$. Orthogonalized atomic orbitals are, however, not as readily visualized as the ordinary atomic orbitals employed in the present treatment.

TABLE I

13 × 13 SECULAR DETERMINANT FOR LnX FOR ARBITRARY DIRECTIONS OF RECIPROCAL SPACE

(x^2-y^2)	(z^2)	(s_c)	(x_c)	(y_c)	(z_c)	(s_a)	(x_a)	(y_a)	(z_a)	(xy)	(xz)	(yz)	
α	0	0	0	0	0	$\sqrt{3}\,\epsilon(C_x - C_y)$	$\sqrt{3}\,i\xi S_x$	$-\sqrt{3}\,i\xi S_y$	0	0	0	0	
	α	0	0	0	0	$\epsilon(2C_z - C_x - C_y)$	$-i\xi S_x$	$-i\xi S_y$	$2i\xi S_z$	0	0	0	
		$\eta + 4\zeta(C_xC_y + C_xC_z + C_yC_z)$	0	0	0	$2\rho(C_x + C_y + C_z)$	$2i\sigma S_x$	$2i\sigma S_y$	$2i\sigma S_z$	$-4\mu S_xS_y$	$-4\mu S_xS_z$	$-4\mu S_yS_z$	
			$\mathscr{D}$	0	0	$2i\mathscr{G}S_x$	$2\mathscr{H}C_x + 2\mathscr{I}(C_y + C_z)$	0	0	0	0	0	
				$\mathscr{D}$	0	$2i\mathscr{G}S_y$	0	$2\mathscr{H}C_y + 2\mathscr{I}(C_x + C_z)$	0	0	0	0	
					$\mathscr{D}$	$2i\mathscr{G}S_z$	0	0	$2\mathscr{H}C_z + 2\mathscr{I}(C_x + C_y)$	0	0	0	
						$k + 4l(C_xC_y + C_xC_z + C_yC_z)$	0	0	0	0	0	0	$= 0$
							p	0	0	0	0	0	
								p	0	0	0	0	
									p	0	0	0	
										$a + 4cC_xC_y + 4eC_z(C_x + C_y)$	0	0	
											$a + 4cC_xC_z + 4eC_y(C_x + C_z)$	0	
												$a + 4cC_yC_z + 4eC_x(C_y + C_z)$	

characterized by direct cation–cation interactions along the ⟨110⟩ directions and into another subset characterized by cation–anion interactions along the ⟨100⟩ directions. This matter is of interest since this classification scheme has been used at least implicitly in all prior work. Examination of the secular determinant indicates that such a step cannot generally be justified. To show this, introduce further simplifications by neglect of† (5) all X–X interactions, (6) all π-type Ln–X interactions, (7) all δ-type or mixed δ interactions characterized by parameters such as E_{xy,z^2} (110), $E_{s_c z^2}$ (110), $E_{z_c z^2}$ (110), $E_{x_c y_c}$ (110), $E_{x_c y_c}$ (110).

The excised secular determinantal equation is shown in Table I. The various symbols are defined in Table II. It is seen that even under the rather drastic approximations just introduced, the determinantal equation fails to split into two parts corresponding to ⟨100⟩– and to ⟨110⟩–type interactions (hereafter termed rectilinear and diagonal-type bonding). Examination shows that the problem resides in the Ln 6*s* orbitals which strongly engage in both types of bonding. A splitting is achieved only by neglect of either (8a) the $E_{s_c s_a}$(100) and $E_{s_c x_a}$(100) or (8b) the $E_{s_c xy}$ (110) parameters. Neither of these possibilities appears physically realistic. If one, nevertheless, proceeds as indicated under (8a) one obtains subbands arising out of (i) interactions among the s_c and the three t_{2g} orbitals participating in diagonal bonding and (ii) interactions among the x^2-y^2, z^2, x_c, y_c, z_c orbitals interacting with the s_a, x_a, y_a, z_a orbitals. Under (8b) the t_{2g} orbitals split off to form three equivalent t_{2g} cation–cation bands, and all remaining orbitals participate in rectilinear bonding. In this particular case the dispersion relations for the t_{2g} bands may be read off from the last three diagonal entries of the table: For the t_{2g} bands in the approximations (5)–(7), and (8b) one finds that (the lattice constant is 2a)

$$\epsilon = E_{xy,xy}(000) + 4E_{xy,xy}(110)\cos(k_x a)\cos(k_y a) + 4E_{xy,xy}(011)\cos(k_z a)[\cos(k_x a) + \cos(k_y a)]$$

specifies the band structure; two additional relations are found by cyclic permutation of the x, y, z subscripts to the **k**-vector. The remaining 10×10 secular determinant for the cation–anion interactions does not simplify further.

Since there seems to be no real justification for introducing condition (8) it is desirable to use other methods which simplify Table I. These consist in deriving the secular determinantal equations for specific directions of high symmetry in reciprocal space, namely the ⟨100⟩ ($k_y = k_z = 0$), ⟨110⟩ ($k_x = k_y \equiv k, k_z = 0$) and ⟨111⟩ ($k_x = k_y = k_z \equiv k$) directions. In each instance one obtains determinants of smaller dimensions which are displayed separately in Tables III–V. These results are obtained by carrying out standard operations in combining rows and columns of the original determinant in Table I, after introducing the simplifications in **k** described above; assumptions (5)–(7) must also be utilized.

† These simplifications are numbered consecutive to those introduced in Section 2.

TABLE II

DEFINITION OF SYMBOLS

Symbol	Parameter	Symbol	Parameter
a	$E_{xy,xy}$ (000)	α	$E_{z z z z}$ (000)
c	$E_{xy,xy}$ (110)	ϵ	$E_{z z s_a}$ (001)
e	$E_{xy,xy}$ (011)	ξ	$E_{z z z_a}$ (001)
k	$E_{s_a s_a}$ (000)	η	$E_{s_c s_c}$ (000)
l	$E_{s_a s_a}$ (110)	ζ	$E_{s_c s_c}$ (110)
p	$E_{x_a x_a}$ (000)	ρ	$E_{s_c s_a}$ (100)
$\mathscr{D}$	$E_{x_c x_c}$ (000)	σ	$E_{s_c x_a}$ (100)
$\mathscr{G}$	$E_{x_c s_a}$ (100)	μ	$E_{s_c, xy}$ (110)
$\mathscr{H}$	$E_{x_c x_a}$ (100)		
$\mathscr{I}$	$E_{y_c y_a}$ (000)		

s_a Anionic wave function of *s*-type character.

s_c Cationic wave function of *s*-type character.

p_a Anionic wave function of *p*-type character; angular dependence given by x_a, y_a, or z_a.

p_c Cationic wave function of *p*-type character; angular dependence given by x_c, y_c, or z_c.

t_{2g} Cationic *d*-type wave function; angular dependence given by xy, xz, or yz.

e_g Cationic *d*-type wave function; angular dependence given by x^2-y^2, or $3z^2-r^2 \equiv z^2$.

$E_{l'_{j'} l_j}(\mathbf{q}) \equiv \sum_{\mathbf{q}} [\langle l'_{j'}|\mathbf{H}|l_j(\mathbf{q})\rangle - \epsilon\langle l'_{j'}|l_{j'}(\mathbf{q})\rangle] S_{j'j}(\mathbf{k},\mathbf{q})$.

$C_\lambda \equiv \cos k_\lambda a$, $S_\lambda \equiv \sin k_\lambda a$, (Lattice constant: 2a)

4. Qualitative Band Structure Scheme

The band scheme offered below is based in Tables III–V. One may generally distinguish the following sets of bands: (a) The 4*f* levels (not included in the tables since they are presumed nonbonding), (b) t_{2g} bands, representing cation–cation bands, of which at least one set is doubly degenerate; these are expected to be relatively narrow as they involve diagonal bonding. (c) Three separate bands deriving from the 3×3 matrix with basis functions p_c, p_a, e_g (in the ⟨100⟩ case the e_g band happens to be split off);

TABLE III

SECULAR DETERMINANTAL EQUATION FOR LnX COMPOUNDS FOR THE ⟨100⟩ DIRECTION IN RECIPROCAL SPACE

$a + 4c + 8eC = 0$ (t_{2g}) $\beta \equiv E_{z^2\,z^2}(110) \to 0$

$a + 4cC + 4e(C+1) = 0$ $(t_{2g}$; doubly degenerate$)$ $\delta \equiv E_{x^2-y^2,\,x^2-yz}(110) \to 0$

$\alpha + 6\beta C + 2\gamma(2+C) = 0$ (e_g)

$$\begin{vmatrix} \mathscr{D} & 2\mathscr{H} + 2\mathscr{I}(1+C) \\ 2\mathscr{H} + 2\mathscr{I}(1+C) & p \\ (p_c) & (p_a) \end{vmatrix} = 0 \text{ (doubly degenerate)}$$

$$\begin{vmatrix} 3\alpha & 0 & 0 & -2\sqrt{3}\,\epsilon(1-C) & 2\sqrt{3}\,i\xi S \\ & \eta + 4\zeta(1+2C) & 0 & 2\rho(2+C) & 2i\sigma S \\ & & \mathscr{D} & 2i\mathscr{G}S & 2\mathscr{H}C + 4\mathscr{I} \\ & & & k + 4l(1+2C) & 0 \\ & & & & p \\ (e_g) & (s_c) & (p_c) & (s_a) & (p_a) \end{vmatrix} = 0$$

these bands arise from strong σ-type overlap between the indicated wave functions. (d) A maximum of six bands arising from primarily σ-type interactions involving the wave functions s_c, p_c, t_{2g}, e_g, s_a, p_a (the t_{2g} band is split off for the ⟨100⟩ case; the e_g state does not participate in this set of band formations in the ⟨11⟩ case).

Diagrams depicting these findings are shown in Figs. 1–3. It must be emphasized that these are highly schematic, but they are satisfactory for the purpose at hand. On the left and right are indicated the atomic cationic and anionic energy levels of the two constituents. In the center are shown the various bands formed through the interactions. These states are designated as f, t_{2g}^{i}, $\sigma_C{}^{i}$, or $\sigma_D{}^{i}$, according as they represent the $4f$ levels or the bands derived from the interactions described in parts (b)–(d) of the preceding paragraph; where appropriate, e_g bands are also sketched in. The index i enumerates successive bands associated with the same secular

TABLE IV

SECULAR DETERMINANTAL EQUATIONS FOR LnX COMPOUNDS FOR THE ⟨110⟩ DIRECTION IN RECIPROCAL SPACE

$a + 4cC + 4eC(1+C) = 0$ $(t_{2g}$; doubly degenerate$)$

$$\begin{vmatrix} \mathscr{D} & 2\mathscr{H} + 4\mathscr{I}C \\ 2\mathscr{H} + 4\mathscr{I}C & p \\ (p_c) & (p_a) \end{vmatrix} = 0$$

$$\begin{vmatrix} \alpha & 0 & 2\sqrt{3}\,i\xi S \\ & 2\mathscr{D} & 4\mathscr{H}C + 4\mathscr{I}(1+C) \\ & & 2p \\ (e_g) & (p_c) & (p_a) \end{vmatrix} = 0$$

$$\begin{vmatrix} \alpha & 0 & 0 & 2\epsilon(1-C) & -2i\xi S & 0 \\ & \eta + 4\xi C(2+C) & 0 & 2\rho(1+2C) & 4i\sigma S & -4\mu S^2 \\ & & 2\mathscr{D} & 0 & 4\mathscr{H}C + 4\mathscr{I}(1+C) & 0 \\ & & & k + 4lC(2+C) & 0 & 0 \\ & & & & 2p & 0 \\ & & & & & a + 4cC^2 + 8eC \\ (e_g) & (s_c) & (p_c) & (s_a) & (p_a) & (t_{2g}) \end{vmatrix} = 0$$

TABLE V

SECULAR DETERMINANTAL EQUATIONS FOR LnX COMPOUNDS FOR THE ⟨111⟩ DIRECTION IN RECIPROCAL SPACE

$$\mathrm{a} + 4\mathrm{c}C^2 + 8eC^2 = 0 \qquad (t_{2g};\ \text{doubly degenerate})$$

$$\begin{vmatrix} 2\mathscr{D} & 0 & 4\mathscr{H}C + 8\mathscr{I}C \\ & \alpha & 2\sqrt{3}\, i\xi S \\ & & 2p \end{vmatrix} = 0 \ \text{(doubly degenerate)}$$

$$\begin{array}{ccccc} (p_c) & (e_g) & (p_a) & & \\ \eta + 12\zeta C^2 & 0 & -12\mu S^2 & 6\rho C & 6i\sigma S \\ & 3\mathscr{D} & 0 & 6i\mathscr{G}S & 6\mathscr{H}C + 12\mathscr{I}C \\ & & 3\mathrm{a} + 12\mathrm{c}C^2 + 24eC^2 & 0 & 0 \\ & & & \mathrm{k} + 12lC^2 & 0 \\ & & & & 3p \\ (s_c) & (p_c) & (t_{2g}) & (s_a) & (p_a) \end{array} = 0$$

determinant in order of increasing energy. The $4f$ levels are actually split by the crystal field but this effect will not be taken into account here. Each band is exactly filled by two valence electrons per formula unit, except where double degeneracies occur which allow occupancy of corresponding bands by four valence electrons per formula unit. The t_{2g}, σ_C and σ_D bands lying near or above the $4f$ levels are probably so closely spaced as to give rise to considerable overlapping, in the manner indicated in Fig. 4.

It is presumed that the band structures exhibited for the directions of high symmetry will remain applicable, with minor adjustment of relative spacing and bandwidths, for arbitrary directions in reciprocal space. In general, the various degeneracies are then also lifted.

5. Correlation with Electrical Properties

The electrical properties to be discussed below may be rationalized by arrangement of the bands as shown in Figs. 1–3. These are drawn so that the four bands derived primarily from the anionic s and p states lie below the $4f$ levels, the latter being on par

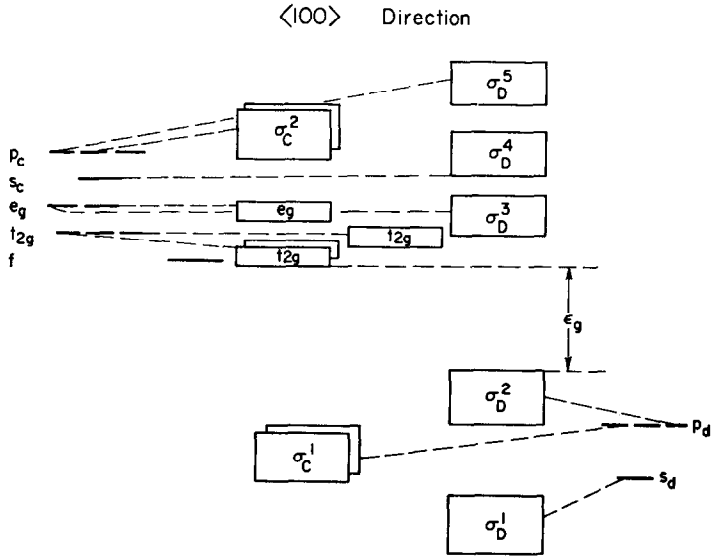

FIG. 1. Schematic diagram for the band structure in LnX along the ⟨100⟩ direction of reciprocal space. The various bands may be correlated with the several secular equations displayed in Table III.

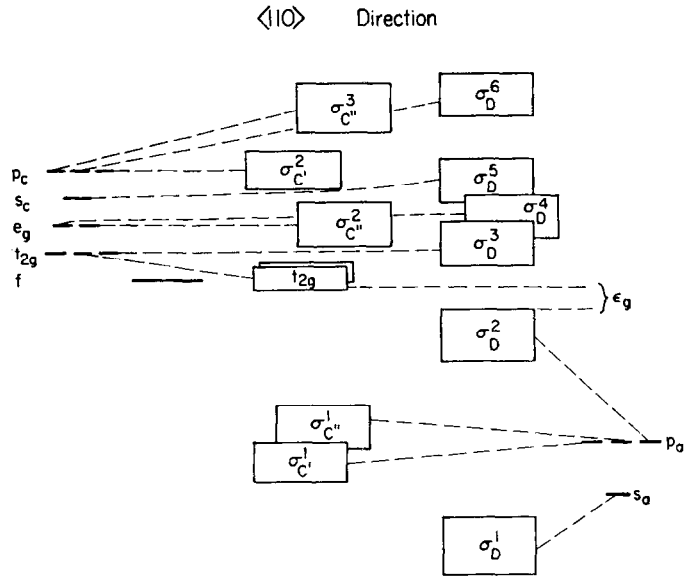

FIG. 2. Schematic diagram for the band structure in LnX along the ⟨110⟩ direction of reciprocal space. The various bands may be correlated with the several secular equations displayed in Table IV.

with the lowest of the sets of levels derived from primarily cationic-type orbitals. This scheme which is rough conformity with the *aufbau* principle of the elements is probably incorrect in detail, though it does not appear to be forced. The energy gap between cationic and anionic bands is designated as ϵ_g.

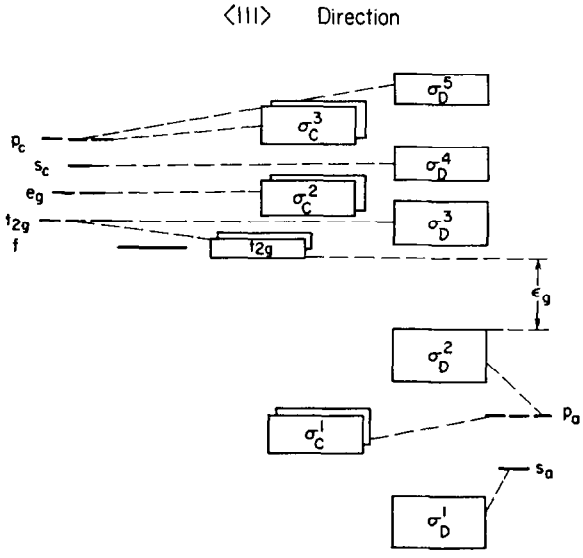

FIG. 3. Schematic diagram for the band structure in LnX along the ⟨111⟩ direction of reciprocal space. The various bands may be correlated with the several secular equations displayed in Table V.

Each formula unit LnX provides five or six electrons deriving from the *ns* and *np* valence shells of the pnicogen or chalcogen, respectively. The lanthanon retains its normal complement of the 4*f* electrons and provides three valence electrons when in the tripositive state, and two if in the dipositive state. Of the above total, eight electrons can be accommodated in the four low-lying bands deriving from the anionic states; the remainder are distributed among the 4*f* states and the low lying t_{2g} or σ_C or σ_D states of primarily *d*-type character.

For chalcogenides with tripositive Ln cations a ninth valence electron must thus be accommodated in a band or a set of bands which remain incompletely filled. The electrical properties of this class of materials is thus readily rationalized. For LnX where the cation is in a dipositive state, an electron is removed from the σ band into the 4*f* level; the material should now be a semiconductor. This appears to be the case for Ln = Sm, Eu, Yb and X = S, Se, Te. In all instances discussed so far it is necessary to place the partially occupied 4*f* levels very close to the Fermi level.

To explain the metallic properties of the pnictides it is necessary to make another assumption, namely that ϵ_g is negative. Thus, at least in some parts of the Brillouin zone, a band which would otherwise be filled is assumed to overlap with one or more bands which would otherwise be empty. As depicted schematically in Fig. 4, this leads to partial occupation of the lower lying band by holes and of the

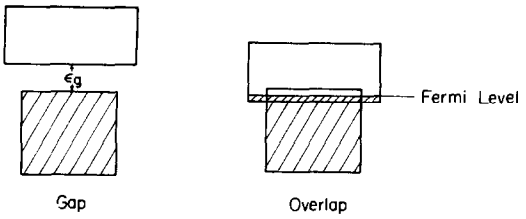

FIG. 4. Diagram illustrating the overlap phenomenon. Shaded area represents filled electron states. Observe simultaneous generation of holes and electrons.

higher lying band(s), by electrons. As before, the partially occupied $4f$ levels lie close to the Fermi level. Under this scheme, all rare earth pnictides should be metallic, as seems indicated by the work cited in Ref. (*8*). However, pnictides of the dipositive lanthanons are reported to have much higher resistivities than pnictides of the tripositive rare earths. For the former the extent of overlapping between bands may be much smaller than for the latter.

The above schemes thus hinge on two postulates. First, to explain the semiconducting characteristics of dipositive lanthanon chalcogenides, a gap must be present which separates the primarily anionic band states from the remainder. Second, to explain the metallic properties of the pnictides, overlapping must occur in at least a limited region of reciprocal space. Since the chalcogenides are likely to be more ionic and thus to have smaller band widths and larger gaps, these postulates seem reasonable. Considerations such as the relative positions of the bands, their widths, and their associated dispersion relations are of importance only when one undertakes a quantitative treatment of the problem.

6. Discussion

Subject to assumptions (1)–(7), the above discussions and tabulations are derived from basic principles inherent in the LCAO-tight binding methodology. Speculations enter only at the point where the relative arrangement of the various bands on the energy scale must be decided. Although this last step is crucial to the interpretation of the data, it is felt that the electrical properties were fitted to a sensible band structure scheme without undue difficulty.

In amplification of earlier statements the following items should be noted: There is experimental evidence that band overlap does occur in some of the rare earth chalcogenides and pnictides. Thus, it is reported (*11*) that the Seebeck coefficient in some of the chalcogenides changes sign as the temperature is altered. This may be ascribed to a variety of factors, but it is also consistent with the overlapping of bands. For, when electrons and holes are simultaneously present, the overall Seebeck coefficient is given by (*14*)

$$\alpha = (-|\alpha_n|\,\sigma_n + \alpha_p\,\sigma_p)/(\sigma_n + \sigma_p)$$

where α_n, α_p are the Seebeck coefficients and σ_n, σ_p the conductivities for electrons and holes. The sign of α is thus determined by a delicate balance between the contribution of electrons to $|\alpha_n|\,\sigma_n$ and of holes to $\alpha_p\sigma_p$. If $|\alpha_n|\,\sigma_n$ rises sufficiently fast with increasing T, α becomes negative in the room temperature range, as is the case with the preponderant majority of the LnX compounds under study. Another fact consistent with the assumed overlapping of bands in the pnictides is the observation (*8*) that YbN has a small negative temperature coefficient of resistivity despite the fact that the material is metallic, as judged by its Seebeck coefficient. This situation can arise if the degree of overlap increases with rising temperature at such a rate that the concomitant increase in carrier densities outweighs the decline in their mobility. Admittedly, considerably more work is required to demonstrate conclusively that required overlapping occurs in the pnictides. One method which has been advocated (*15*, *16*) for this purpose involves measurements of magnetoresistance as a function of magnetic field. In most cases one can thus arrive at an unambiguous decision whether holes and electrons in approximately equal concentrations are simultaneously present.

One should also note that assumption (6) concerning the neglect of π-type interactions is always risky. For, it frequently happens in σ-type bonding that a very diffuse cationic wave function covers the positive and negative lobes of a less diffuse anionic wave function almost to the same extent. In this case, the assumption that π-type E parameters are smaller than σ-type E parameters may not hold. However, it has been verified by the author that abandonment of assumption (6), while somewhat altering the entries in Tables III–V, does not invalidate the scheme of Figs. 1–3 and does not invalidate the conclusions drawn here.

Finally, it is evident that in favorable instances, the present approach provides *analytic* solutions for the band structures. Thus, there is no problem in obtaining the $\epsilon(\mathbf{k})$ dependence for the 1×1 and 2×2 entries of Tables III–V. Even for higher order determinants the situation is by no means hopeless, provided only that the various E parameters in off-diagonal entries are small compared to the

differences in energy corresponding to the diagonal entries they connect. For, one may then use standard first and second order perturbation theory for approximate diagonalization of these higher order determinants. The specification of analytic solutions is a significant advance over the schematic presentation of the data, and represents an alternative approach to numerical machine calculations. Furthermore, knowing the $\epsilon(\mathbf{k})$, one can make detailed predictions concerning transport properties. The above material represents a first step in this direction.

References

1. E. F. Westrum, Jr., *in* "Progress in the Science and Technology of the Rare Earths" (L. Eyring, ed.). Pergamon, Oxford, Vol. 2, p. 35 (1966) and Vol. 3, p. 459 (1968).
2. R. Lallement and J. J. Veyssie, *in* "Progress in the Science and Technology of the Rare Earths" (L. Eyring, ed.). Pergamon, Oxford, Vol. 3, p. 284 (1968).
3. J. C. Slater and G. F. Koster, *Phys. Rev.* **94**, 1498 (1954).
4. H. Bilz, *Z. Physik* **153**, 338 (1958).
5. J. M. Honig, J. O. Dimmock, and W. Kleiner *J. Chem. Phys.*, in press.
6. E. Rundle, *Acta Cryst.* **1**, 180 (1948).
7. H. Krebs, *Acta Cryst.* **9**, 95 (1956).
8. R. Didchenko and F. H. Gortsema, *J. Phys. Chem. Solids* **24**, 863 (1963).
9. J. W. McClure, *J. Phys. Chem. Solids* **24**, 871 (1963).
10. V. I. Marchenko and G. V. Samsonov, *Russ. J. Inorg. Chem.* **8**, 1061 (1963).
11. V. P. Zhuze, A. V. Golubkov, E. V. Goncharova, T. I. Komarova, and V. M. Sergeeva, *Soviet Physics-Solid State* **6**, 213 (1964); V. P. Zhuze, A. V. Golubkov, E. V. Goncharova, and V. M. Sergeeva, *ibid.* **6**, 205 (1964); A. V. Golubkov, E. V. Goncharova, V. P. Zhuze, and I. G. Manoilova *ibid.* **7**, 1963 (1966).
12. J. B. Goodenough, *Bull. Soc. Chim. France* **1965**, 1200; *Czechoslovak J. Phys.* **B17**, 304 (1967).
13. J. Callaway, "Energy Band Theory." Academic Press, New York (1964).
14. T. C. Harman and J. M. Honig, "Thermoelectric and Thermomagnetic Effects and Applications." McGraw-Hill, New York (1967).
15. C. H. Champness, *Can. J. Phys.* **41**, 890 (1963).
16. J. M. Honig and T. B. Reed, *Phys. Rev.* **174**, 1020 (1968).